Neuropharmacology 259 (2024) 110120

Contents lists available at ScienceDirect

Neuropharmacology

journal homepage: www.elsevier.com/locate/neuropharm

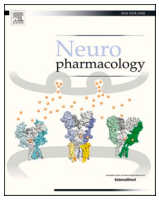

Neuroinflammation evoked mechanisms for neuropathic itch in the spared nerve injury mouse model of neuropathic pain

Vittoria Borgonetti [1], Martina Morozzi [1], Nicoletta Galeotti [*]

Department of Neurosciences, Psychology, Drug Research and Child Health (Neurofarba), University of Florence, Viale G. Pieraccini 6, Florence, Italy

ARTICLE INFO

Keywords:
Neuropathic pain
Neuropathic itch
Spared nerve injury
B-type natriuretic peptide
Interleukin 17

ABSTRACT

A large portion of neuropathic pain suffering patients may also concurrently experience neuropathic itch, with a negative impact on the quality of life. The limited understanding of neuropathic itch and the low efficacy of current anti-itch therapies dictate the urgent need of a better comprehension of molecular mechanisms involved and development of relevant animal models. This study was aimed to characterize the itching phenotype in a model of trauma-induced peripheral neuropathy, the spared nerve injury (SNI), and the molecular events underlying the overlap with the nociceptive behavior. SNI mice developed hyperknesis and spontaneous itch 7–14 days after surgery that was prevented by gabapentin treatment. Itch was associated with pain hypersensitivity, loss of intraepidermal nerve fiber (IENF) density and increased epidermal thickness. In coincidence with the peak of scratching behavior, SNI mice showed a spinal overexpression of IBA1 and GFAP, microglia and astrocyte markers respectively. An increase of the itch neuropeptide B-type natriuretic peptide (BNP) in NeuN+ cells, of its downstream effector interleukin 17 (IL17) along with increased pERK1/2 levels occurred in the spinal cord dorsal horn and DRG. A raise in BNP and IL17 was also detected at skin level. Stimulation of HaCat cells with conditioned medium from BV2-stimulated SH-SY5Y cells produced a dramatic reduction of HaCat cell viability. This study showed that SNI mice might represent a model for neuropathic itch and pain. Collectively, our finding suggest that neuropathic itch might initiate at spinal level, then affecting skin epidermis events, through a glia-mediated neuroinflammation-evoked BNP/IL17 mechanism.

1. Introduction

Neuropathic pain is a chronic disabling condition (Finnerup et al., 2021) that is frequently associated with several comorbidities which further adversely affect the quality of life of patients (Bushnell et al., 2013; Woo, 2010). Apart from sensory abnormalities, chronic pain alters mood and impairs cognitive functions. Severe neuropathic pain patients show a prevalence for the development of depression and anxiety symptoms five times higher than in the general population (Rayner et al., 2016). Memory and cognitive dysfunctions are also frequently observed (Dick and Rashiq, 2007). Neuropathic patients may also concurrently experience pain and itch (Hachisuka et al., 2018). About 90% of patients with small fiber neuropathies (Pereira et al., 2020a) and 30–65% of post-herpetic zoster patients experience both neuralgia and itch (Oaklander et al., 2003).

Pathophysiologically, itch can be classified as dermatological, systemic, psychologic and neuropathic (Ständer and Grundmann, 2013). Neuropathic itch accounts for approximately 8%–19% of chronic pruritus conditions and can be developed in several diseases characterized by a damage or dysfunction of the peripheral or central nervous system (Cevikbas and Lerner, 2020a; Stumpf and Ständer, 2013). The main symptoms of neuropathic itch are represented by alloknesis (itch sensation by a non-pruritic stimulation) and hyperknesis (increased itch in response to a touch stimulation) (Andersen et al., 2018). These dysesthesias closely resemble to the neuropathic pain associated symptoms allodynia and hyperalgesia. Indeed, pain and itch are distinct, but related sensations: both of them are involved in the protection from a potential external damage (Basbaum et al., 2009; Cevikbas and Lerner, 2020a) by driving different behavioral responses. A pruritic stimulus evokes a scratching reflex (Wimalasena et al., 2021) while a nociceptive stimulus evokes a withdrawal behavior (Ma, 2022). These two sensations also share similar anatomical ascending pathways (Ikoma et al., 2006; Liu and Ji, 2013). Pain- and itch-detecting neurons are small-diameter, unmyelinated C-fibers of the dorsal root ganglia and

* Corresponding author. Department of Neurofarba, Viale G. Pieraccini 6, 50139, Florence, Italy.
E-mail address: nicoletta.galeotti@unifi.it (N. Galeotti).
[1] Equal contribution.

https://doi.org/10.1016/j.neuropharm.2024.110120
Received 27 April 2024; Received in revised form 11 August 2024; Accepted 16 August 2024
Available online 17 August 2024
0028-3908/© 2024 The Authors. Published by Elsevier Ltd. This is an open access article under the CC BY license (http://creativecommons.org/licenses/by/4.0/).

trigeminal ganglia that synapse in the outer layers of the dorsal horn of the spinal cord (Steinhoff et al., 2006). Under physiological conditions, an antagonistic interaction between pain and itch is usually observed. Conversely, under pathological conditions pain and itch share numerous mechanistic similarities (Cevikbas and Lerner, 2020a).

The pathophysiological consequences of neuropathic itch impact quality of life as much as neuropathic pain. However, while intense research has been devoted to understand the mechanisms involved in neuropathic pain to the development of new therapies, the etiology of neuropathic itch is still poorly understood and lacks approved therapy (Poddar et al., 2023; Steinhoff et al., 2018). In fact, the drug therapies available to date for this form of chronic itching are very limited. Thus, it is necessary to investigate this form of spontaneous onset itching in animals' model of neuropathic pain. In fact, peripheral neuropathy is the most common etiology of neuropathic itch (Rosen et al., 2018). For this reason, this study was aimed to characterize the itching phenotype in a model of trauma-induced peripheral neuropathy, the spared nerve injury (SNI) and correlated it with the onset of nociceptive behavior. Moreover, we investigated the alteration of factors involved in both itching (BNP, epidermal thickness) and chronic pain (neuroinflammation, IENF) occurring in the skin, DRG and spinal cord so that we could understand the possible correlation between these two processes. Finally, we optimized an in vitro model using keratinocyte cells (HaCat), neuronal cells (SH-SY5Y), and microglial cells (BV-2) to mimic the molecular events observed in SNI animals.

2. Materials and methods

2.1. Animals

CD1 male mice (6 weeks old) weighting approximately 20 g (Envigo, Varese, Italy) were housed in the Ce.S.A.L. (Centro Stabulazione Animali da Laboratorio, University of Florence) vivarium and used 3 days after their arrival. Mice were housed in standard cages, kept at 23 6 1 °C with a 12-h light/dark cycle, light on at 7 a.m., and fed with standard laboratory diet and tap water ad libitum. All tests were conducted during the light phase. The experimental protocol was approved by the Institution's Animal Care and Research Ethics Committee (University of Florence, Italy), under license from the Italian Department of Health (54/2014-B). Mice were treated in accordance with the relevant European Union (Directive, 2010/63/EU, the council of September 22, 2010, on the protection of animals used for scientific purposes) and international regulations (Guide for the Care and Use of Laboratory Animals, US National Research Council, 2011). All studies involving animals are reported in accordance with the ARRIVE 2.0. The experimental protocol was designed to minimize the number of animals used and their suffering. The G power software was used to perform a power analysis to choose the number of animals per experiment (Charan and Kantharia, 2013).

2.2. Drug administration

Mice were randomly assigned to each treatment group by an individual other than the operator. Pregabalin (30 mg/kg i.p.) (Sigma, Milan, Italy) was dissolved in saline solution and administered 3 h before testing and experiments were conducted by operators blinded to the treatment of the animals.

2.3. Spared nerve injury procedure

The SNI model represents a peripheral mononeuropathy model that was performed as previously described (Decosterd and Woolf, 2000). Briefly, the animals were anaesthetized with 4% isoflurane in O_2/N_2O (30:70 vol/vol). The right paw, conventionally called "ipsi," was operated, whereas the left "contra" remained intact. A skin incision was made laterally on the right limb to identify the sciatic nerve. Of the 3 branches of the nerve, the common peroneal and tibial were tied together with 5.0 silk suture thread (Ethicon; Johnson & Johnson Intl, Brussels, Belgium) and cut, with the sural remaining intact. Tests were then conducted 3 days after the operation to detect the postsurgical appearance of mechanical allodynia and thermal hyperalgesia. The experimental groups were control (Sham) mice (n = 21; sham-operated mice) and SNI mice (n = 25; operated mice) subdivided into 2 different cohorts of animals. Sham mice underwent the same surgical procedure without ligation and transection of the nerves. Sex differences in response to pain have been described in the SNI model in which microgliosis and pain hypersensitivity were mainly detected in male mice (Ann M. Gregus et al., 2021).

2.4. Behavioral studies

2.4.1. Scratching behavior

To evaluate the spontaneous scratching behavior induced by SNI, behavioral experiments were performed on post-surgical day 7, 14 and 21. Mice were habituated in plastic cages (78 × 60 × 39 cm) for 60 min before testing. The number of scratching bouts in 10 min was counted. A scratching bout was defined when a mouse lifted its hind paw to scratch the trunk or nape areas of the body and returned the paw to the floor or to the mouth for licking. Analyses were carried out in a blinded fashion.

2.4.2. Hyperknesis assay

Hyperknesis, defined as itching evoked by a mechanical stimulus, was evaluated on day 7, 14 and 21 post-surgery. On the day of the test mice were placed in individual cages for habituation for 30 min. Hyperknesis was induced by a von Frey filament (bending force of 2.0 g) applied to the central part of the back. A scratching bout directed to the site of mechanical stimulation was considered as a positive response. The hyperknesis score was determined by calculating time spent by the animal on scratching after the application of the mechanical stimulus in 30 s.

2.4.3. Mechanical allodynia

Mechanical allodynia was determined as the force (g) required to elicit the withdrawal of a paw from the applied stimulus with the use of von Frey monofilaments. The up–down protocol was applied in which a lack of response to a filament requires the use of the next higher filament in the following stimulation. After adaptation for approximately 1 h, filaments (0.07, 0.16, 0.4, 0.6, 1.0, 1.4 and 2.0 g) were applied in the injured (ipsilateral) leg. Measurements from the uninjured (contralateral) leg were used as control values. The test was performed before SNI and on day 7, 14, and 21 after surgery (Borgonetti and Galeotti, 2021).

2.4.4. Thermal hyperalgesia

To assess thermal hyperalgesia, the hot-plate test was used. Each mouse is placed individually on the metal surface of the apparatus (24 cm diameter), maintained at the constant temperature of 52 °C, which is surrounded by a transparent acrylic cage. The time (s) taken to elicit a nocifensive behavior (e.g., paw withdrawal or licking or shaking, jumping) is recorded. The test was performed before SNI and on day 7, 14, and 21 after surgery (Borgonetti and Galeotti, 2021).

2.4.5. Open field test

The open field test is used to assess the anxiety-like behavior of SNI mice. The animal is placed into the center of a rectangular box (78 × 60 × 39 cm) surrounded by walls, in which an internal perimeter (3 cm from the walls) is traced. The time each animal remains in the internal portion is measured over a 5 min period. Mice prefer not to remain in the center area of the box that represents a novel and stressful environment to the animal. The longer the animal stays next to the walls, the more anxious-like it is. The test was performed before SNI and on day 7, 14, and 21 after surgery (Borgonetti and Galeotti, 2023).

2.5. Tissue analysis

2.5.1. Protein lysates from tissue

Spinal cord, dorsal root ganglia (DRG) and dorsal skin samples from sham and SNI mice were homogenized in a lysis buffer containing 25 mM Tris-HCl pH (7.5), 25 mM NaCl, 5 mM EGTA, 2.5 mM EDTA, 2 mM NaPP, 4 mM PNFF, 1 mM Na_3VO_4, 1 mM PMSF, 20 μg/mL leupeptin, 50 μg/mL aprotinin, 0.1% SDS. The homogenate was centrifuged at 12,000×*g* for 30 min at 4 °C and the pellet was discarded. The total protein concentration in the supernatant was measured using Bradford colorimetric method.

2.5.2. Western blotting analysis

Protein samples (10 μg of protein/lane) were separated by 10% SDS-polyacrylamide gel electrophoresis (SDS-PAGE). Proteins were then blotted onto nitrocellulose membranes (90 min at 110 V) using standard procedures. Membranes were blocked in PBST (PBS with 0.1% Tween) containing 5% non-fat dry milk for 90 min and incubated overnight at 4 °C with primary antibody against BNP (1:500); IL-17 (1:1000), phosphorylated ERK1/2 (1:1000) (Santa Cruz Biotechnology, Santa Cruz, CA). The day after, blots were rinsed three times with PBST and incubated for 2 h at rt with HRP-conjugated secondary antibodies and then detected by a chemiluminescence detection system (Life Technologies Italia, Monza, Italy) (Galeotti et al., 2001). Signal intensity (pixels/mm^2) was quantified using ImageJ (NIH). The signal intensity was normalized to the total protein content.

2.5.3. Immunofluorescence analysis on tissue

Spinal cord, DRG, dorsal skin and glabrous plantar skin of the hind paw samples were fixed in formalin at 4% for 24 h, dehydrated in alcohol, included in paraffin. Paraffin blocks were cut into 20 μm sections, except for blocks of plantar skin that were cut into 15 μm sections. The primary antibody used were against BNP (1:100), GFAP (1:300), IL-17 (1:100) (Santa Cruz Biotechnology), CD11b (1:200) (Bioss Biotach), NeuN (1:200) (Cell Signaling Biotec), PGP 9.5 (1:5000) (Biogenesis), diluted in 1% BSA in PBS overnight at 4 °C. After rinsing in PBS containing 0.01% Triton-X-100, sections were incubated in secondary antibodies Invitrogen Alexa Fluor 488 (490–525, 1:400), Invitrogen Alexa Fluor 568 (1:400) (Thermo Fisher Scientific, Waltham, MA), and Cruz Fluor 594 (1:400) (Santa Cruz Biotechnology) at rt for 2 h. Sections were coverslipped using Vectorshield mounting medium (Vector Laboratories, Burlingame, CA). Images were acquired with an OLYMPUS BX63F fluorescence microscope connected to a PC with an image acquisition card. The immunofluorescence intensity was calculated using Image J.

2.5.4. Hematoxylin and eosin staining

The dorsal skin samples were fixed in 4% formalin solution for 24 h, repeatedly rinsed, dehydrated, embedded in paraffin solution, and cut into 10-μm sections. Deparaffined skin sections were stained with 5% hematoxylin and 1% eosin (H&E). The slides were observed on a Nikon ECLIPSE TS2-S-SM and the skin thickness was determined. Images were analyzed using ImageJ and using black and white.

2.6. Cell culture studies

2.6.1. BV2 Cell culture

BV2 murine immortalized microglial cells (mouse, C57BL/6, brain, microglial cells, Tema Ricerca, Genova, Italy; 16–20 passages) were used. The cells were thawed and placed in a 75 cm^2 flask (Sarstedt, Milan) in a medium containing Roswell Park Memorial Institute (RPMI) media with the addition of 10% of heat-inactivated (56 °C, 30 min) fetal bovine serum (FBS, Gibco®, Milan) and 1% glutamine. Cells were grown at 37 °C and 5% CO_2 with daily medium change. Microglial cells were seeded in 6-well plates (3×10^5 cells/well) until 70–80% confluence was achieved. To induce microglial cell activation, BV2 were stimulated with LPS, (250 ng/ml) for 72 h.

2.6.2. SH-SY5Y cell culture

A human neuroblastoma cells (SH-SY5Y, passages 6–20, Cat# 94,030,304 ECACC), were cultured in 25 cm^2 cell culture flasks in 1:1 Dulbecco's Modified Eagle Medium (DMEM; Merck, Darmstadt, Germany) and F12 Ham's nutrients mixture (Merck), containing 10% heat-inactivated FBS (Merck), 1% L-glutamine (Merck), and 1% penicillin–streptomycin solution (Merck) until confluence (70%–80%). Cells were exposed to unstimulated or LPS-stimulated BV2 conditioned medium for 48 h.

2.6.3. HaCat cell culture

HaCaT (immortalized human keratinocytes) cells were a gift from Prof. Monica Montopoli (University of Padua, Italy). Cells were cultured on 75 cm^3 cell culture flasks and grew in Dulbecco's modified Eagle's medium - high glucose (1:1), L-glutamine (1%) containing 10% fetal bovine serum (FBS) and 1% antibiotic Pen-Strep (1%). Cells were grown at 37 °C in 5% CO_2 to achieve 70–80% confluency, with medium changed daily. Cells were exposed to SH-SY5Y conditioned medium for 48 h previously exposed to unstimulated or LPS-stimulated BV2 conditioned medium. The effect of cytotoxicity on HaCat of BV2 and SH-SY5Y co-culture medium was measured by doing cell counts, using ImageJ.

2.6.4. Immunofluorescence staining on SH-SY5Y

Cells were fixed with 4% paraformaldehyde (PFA) for 15 min at rt. Following incubation with blocking buffer (PBS, containing 1% bovine serum albumin) for 1 h at rt, primary antibody against NBP (1:500 in PBSA 5%; Santa Cruz Biotechnology) was added for 2 h at rt. Primary antibody was removed and fixed cells were incubated in secondary antibodies labeled with Invitrogen Alexa Fluor 568 (578–603, 1:500; Thermo Fisher Scientific) for 1 h. Samples were coverslipped using UltraCruz® Aqueous Mounting Medium with DAPI (Santa Cruz Biotechnology) to identify the nucleus. Images were acquired with a Leica DM6000B fluorescence microscope. The immunofluorescence intensity was calculated by Image J (NIH).

2.7. Statical analysis

All data are presented as the mean ± SEM. Biochemical and behavioral data were analyzed using one-way or two-way ANOVA followed by Tukey's or Bonferroni's post hoc test, respectively. The criterion for statistical significance was a P value of less than 0.05. Statistical analyses were conducted with GraphPad Prism 10 (GraphPad Software).

3. Results

3.1. SNI behavioral phenotype

3.1.1. Scratching behavior in SNI mice

To define the itching phenotype of SNI mice, the scratching behavior was evaluated at different time points after surgery (Fig. 1A). Results were compared to those from sham mice to exclude that the scratching behavior was related to the surgical procedure or healing process. SNI mice showed an early hyperknesis as indicated by the increase in the mechanically evoked scratching time that was significant starting from day 7 post-injury. Itch peaked on day 14 then diminished and disappeared on day 21 post-surgery, showing values comparable to the sham group (Fig. 1B and C). SNI mice also showed spontaneous itch. The evaluation of the number of spontaneous scratching bouts showed a trend toward an increase on day 7. A peak of scratching behavior was observed on day 14 while the effect disappeared on day 21 (Fig. 1C and D). Interestingly, the spontaneous itch was detectable in the morning (9.00 a.m.), but not in the evening (5.00 p.m.) (Fig. 1E).

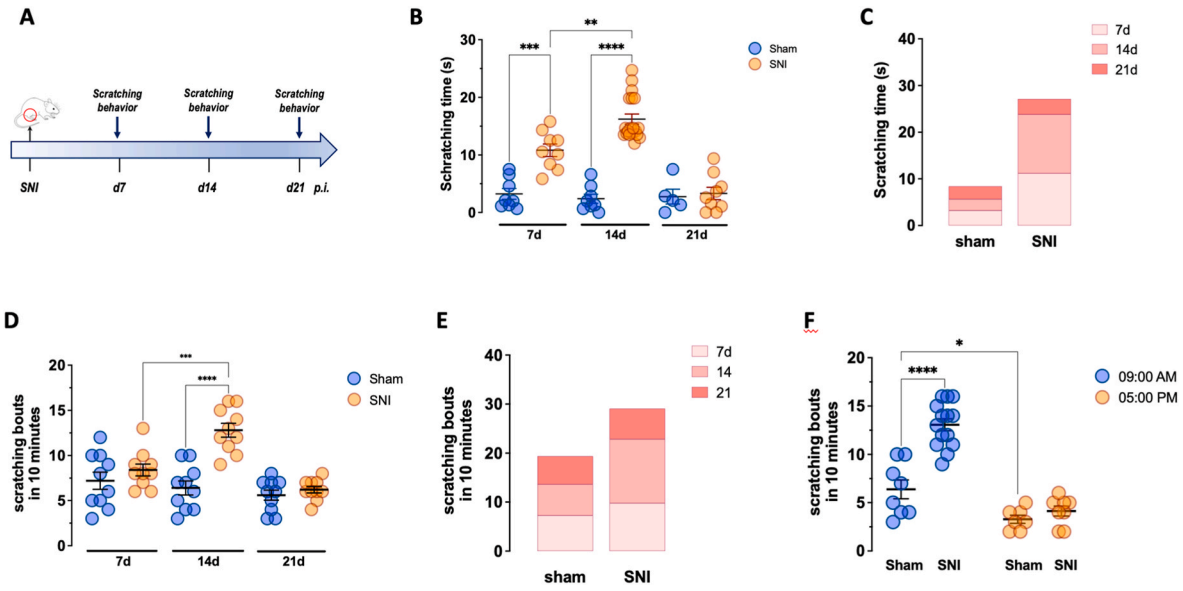

Fig. 1. Scratching behavior in SNI mice. (**A**) Schematic representation of the experimental protocol. (**B**) Time-course evaluation of the mechanically evoked scratching behavior in SNI mice evidencing an increase in the scratching time 7- and 14-days post-surgery. **(C)** Cumulative scratching behavior induce by a mechanical stimulus. (**D**) Time-course evaluation of the spontaneous scratching behavior showed a peak of scratching bouts on day 14 post SNI. (**E**) Cumulative number of spontaneous scratching bouts in SNI mice. (**F**) Different spontaneous scratching behavior in SNI mice at 9.00 a.m. and 5.00 p.m. *P < 0.05, **P < 0.01, ***P < 0.001, ****P < 0.0001 (two-way ANOVA).

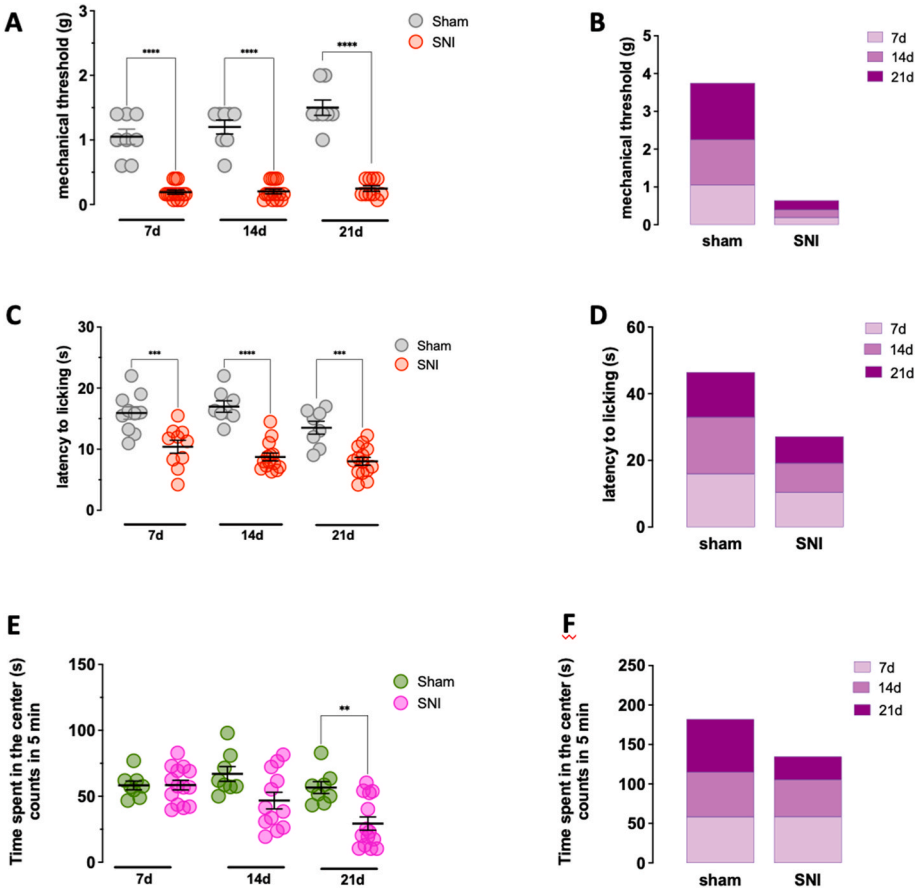

Fig. 2. Nociceptive and anxiety-like behavior of SNI mice. (A) Time course and (B) cumulative evaluation of mechanical allodynia by von Frey test in SNI mice monitored on day 7, 14 and 21 post-surgery. (C) Time course and (D) cumulative monitoring of thermal hyperalgesia by means of the hot plate test in SNI mice (day 7, 14 and 21 post-surgery). (E) Evaluation of anxiety-like behavior and (F) cumulative response in the open field test in SNI mice. **P < 0.01, ***P < 0,001, ****P < 0.0001 (two-way ANOVA).

3.1.2. SNI mice nociceptive phenotype

To further characterize the itching phenotype of SNI mice and to assess the potential overlap with pain hypersensitivity, the nociceptive behavior was evaluated. As expected, mice showed a severe and long-lasting pain hypersensitivity. A drastic drop in the reaction to a mechanical stimulus was observed in the ipsilateral side from day 7 post-injury that persisted unaltered up to day 21 (Fig. 2A and B). Similarly, mice showed a persistent thermal hypersensitivity that was significant from day 7 to day 21 with a comparable intensity at all time points (Fig. 2C and D). These results highlighted an overlap of the scratching and nociceptive behavior on day 7 and 14.

3.1.3. Anxiety-like behavior of SNI mice

Neuropathic pain is accompanied by several comorbidities, including alteration of mood. Furthermore, a correlation between anxiety and itch has been observed (Sanders and Akiyama, 2018). We, thus, investigated whether SNI mice might develop an anxiety-like behavior. Results from the open field test showed the lack of effects on day 7 on SNI mice in comparison with sham mice. On day 14 there was a decrease in the time spent in the center of the arena, taken as an index of anxiety-like behavior, that became statistically significant on day 21 (Fig. 2E and F).

3.1.4. Pregabalin suppression of nociceptive and scratching behavior

Pregabalin is a first-line treatment for neuropathic pain in clinics (Attal and Bouhassira, 2021) that have been observed to produce some relief for neuropathic itch (Matsuda et al., 2016). Pregabalin (30 mg/kg i.p.) was administered on day 14 post-surgery, in coincidence to the peak of scratching behavior and the effects were evaluated 3 h after treatment. SNI mice were highly responsive to gabapentin. Treated mice showed a reduced spontaneous itch (Fig. 3A) and hyperknesis (Fig. 3B). In the same experimental conditions pregabalin resulted effective in reducing the hypernociceptive behavior as it abolished mechanical allodynia (Fig. 3C) and thermal hyperalgesia (Fig. 3D).

3.2. Altered peripheral innervation and epidermis morphology in SNI mice

Decrease of the intraepidermal nerve fiber (IENF) density in the skin is a characteristic trait of mouse models of peripheral neuropathies (Klazas et al., 2022; Sanna et al., 2020). We detected the IENF in the glabrous hind paw skin in SNI mice by immunofluorescence staining of PGP9.5, a pan-neuronal marker used to quantify fibers crossing the dermal-epidermal junction (Fig. 4A). Consistent with our previous results (Sanna et al., 2018), quantification analysis showed a reduction of approximately 60% on day 14 and 50% on day 21 post-injury compared with that of control sham mice (Fig. 4B).

A time-dependent morphological alteration of the epidermis was detected in SNI mice. Microscopic observation of the dorsal skin sections revealed significant differences between SNI and sham mice. Skin samples showed a variation in the epidermis thickness (Fig. 4C). Quantification analysis confirmed that the average epidermal thickness in SNI mice was increased compared to sham on day 14 and 21 post-injury with a peak effect on day 14 (Fig. 4D).

3.3. BNP upregulation in lumbar dorsal root ganglia and spinal cord tissue of SNI mice

An increased expression of BNP was observed in spinal cord samples of SNI, compared to sham mice, on day 14 post-injury. Then the protein levels diminished on day 21 showing a time course comparable to the scratching behavior (Fig. 5A). Immunofluorescence images confirmed this effect in SNI mice, as showed by an increased BNP immunostaining in spinal cord sections on day 14 and 21 post-surgery (Fig. 5B). By comparing the expression in the dorsal and in the ventral horn of SNI spinal cord sections, quantitative analysis showed that BNP protein was more abundantly expressed in the dorsal horn (Fig. 5C). Double staining immunofluorescence experiments in spinal cord sections showed the expression of BNP in NeuN expressing cells that was increased on day 14 and then diminished on day 21 (Fig. 1 Supplementary).

Cellular events involved in the BNP-mediated pathway were investigated. Determination of the levels of IL-17 showed a significant increase on day 14 in spinal cord samples (Fig. 5D). To study functional effects of IL-17 at neuronal sites, the levels of pERK1/2 were determined and results showed a pERK1/2 overexpression for both isoforms (Fig. 5E and F). Similar findings were observed in DRG samples (Fig. 5G,H,I) with a peak on day 14 and a decrease on day 21, showing a time-course overlapping the scratching behavior.

3.4. Glial cell activation in the spinal cord of SNI mice

Growing evidence indicates an important role of spinal glia in the modulation of both pain and itch (Tsuda, 2018). Consistently, in the ipsilateral side of SNI mice an increased immunostaining of CD11b, a marker of microglia, was observed on day 14 and 21 post-surgery (Fig. 6A). Quantification analysis showed a more intense increase on day 14 that then attenuated on day 21 (Fig. 6B). Similarly, an increased immunostaining of the astrocyte marker GFAP was detected in the ipsilateral side (Fig. 6C) that was further confirmed by quantification analysis (Fig. 6D).

3.5. In vitro evaluation of the neuroinflammation-mediated toxicity on the epidermis

To evaluate whether spinal glia activation might promote BNP overexpression to initiate itch sensation that is further amplificated in the skin, we used a cell culture model (Fig. 7A). BV2 microglial cells were stimulated with LPS (250 ng/ml). After 72 h stimulation, the conditioned medium was collected and SH-SY5Y neuroblastoma cells were exposed to the BV2 medium for 48 h. Immunofluorescence staining showed that stimulated SH-SY5Y cells presented a higher BNP expression (Fig. 2 Supplementary). Then, the conditioned medium of stimulated SH-SY5Y cells was collected and added to keratinocytes cells (HaCat). After 48h stimulation, the cell counting of HaCat cells was evaluated.

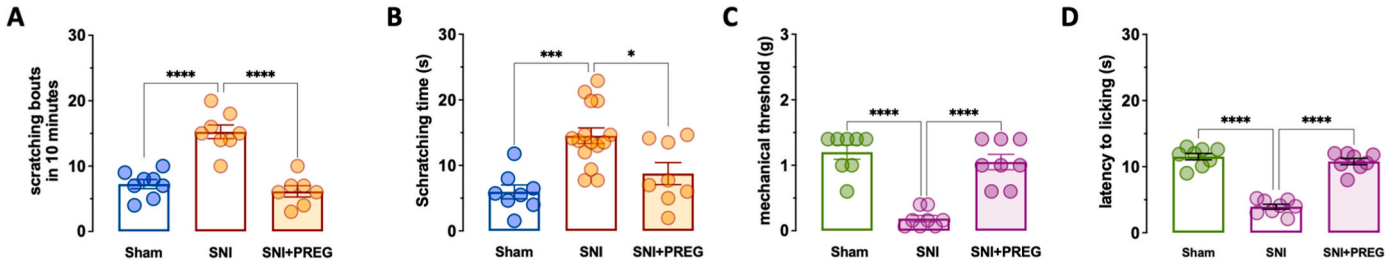

Fig. 3. Effect of pregabalin on nociceptive and scratching behavior. Effect of pregabalin (PREG; 30 mg/kg i.p.) on spontaneous itch, evaluated with (A) scratching bouts in 10 min and hyperknesis (B). Effect of pregabalin on neuropathic pain symptoms: (C) mechanical allodynia and (D) thermal hyperalgesia in SNI mice on day 14 post-surgery. *P < 0.05, ***P < 0,001, ****P < 0.0001 (one-way ANOVA).

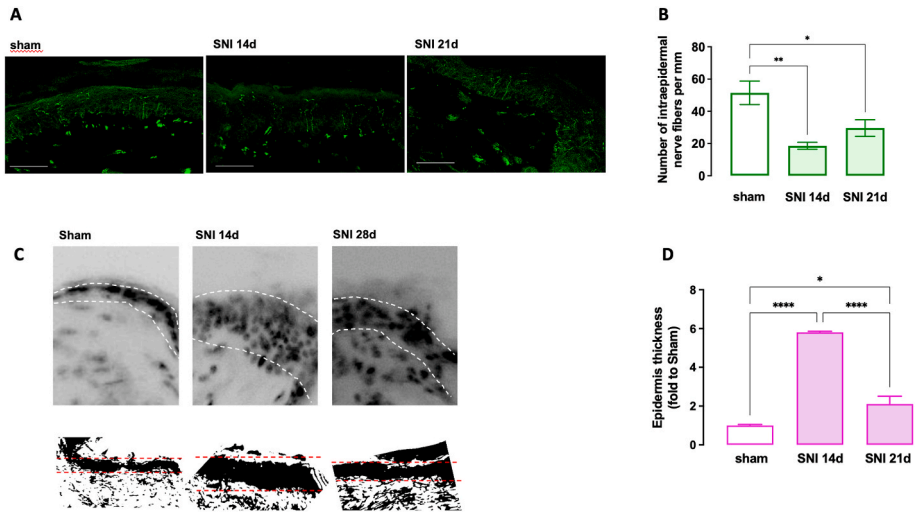

Fig. 4. Peripheral innervation and epidermis morphology of SNI mice. (A) Representative images of the immunofluorescence staining of the intraepidermal nerve fiber (IENF) of the glabrous hind paw skin in SNI mice on days 14 and 21 post-injury compared with that of control sham mice. The sections were immunostained with PGP9.5. Scale bar: 50 μm. (B) Quantification analysis of the IENF in SNI showed a downregulation on day 14 and 21 compared to sham mice. *P < 0.05 (one-way ANOVA). (C) Representative images of dorsal back skin samples from sham, SNI mice on day 14 post-injury and SNI mice on day 21 post-injury stained using hematoxylin and eosin (black and white images); scale bar: 100 μm. (D) Evaluation of epidermis thickness showing a robust increase in SNI on day 14 that was significantly reduced on day 21. *P < 0.05. ***P < 0.001, ****P < 0.0001.

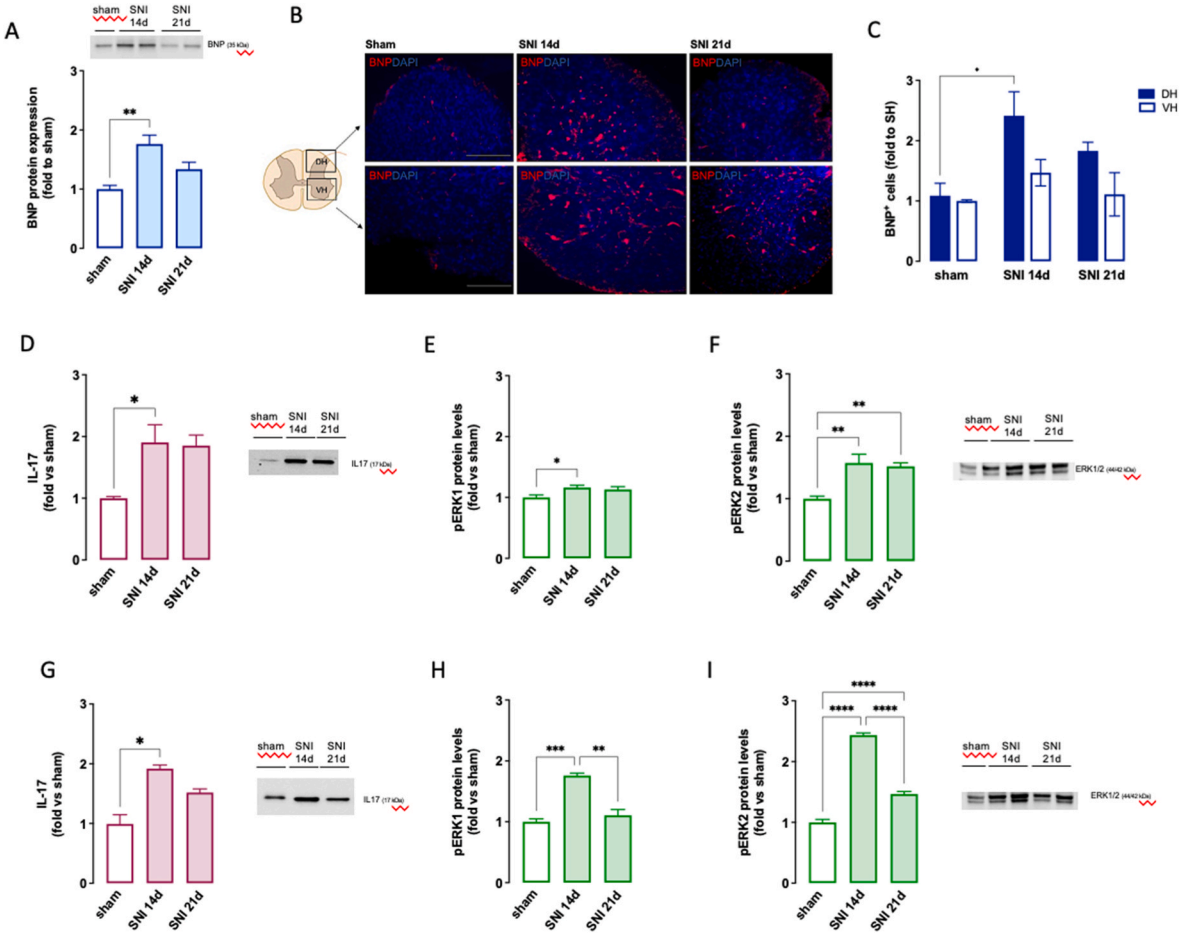

Fig. 5. BNP expression in SNI mice. (A) Spinal BNP protein expression. (B) Immunofluorescence images showing the immunostaining of BNP in the dorsal and ventral horn of the spinal cord of SNI mice on day 14 and 21 post-surgery. Scale bar 100 μM. (C) Quantification analysis of BNP positive cells in the spinal cord dorsal and ventral horn of SNI mice. Nuclei are stained with DAPI. *P < 0.05 (two-way ANOVA). IL17 and pERK1/2 protein expression in spinal cord (D,E,F) and DRG (G,H, I) samples. *P < 0.05, **P < 0.01 ***P < 0.002, ****P < 0.0001 (one-way ANOVA).

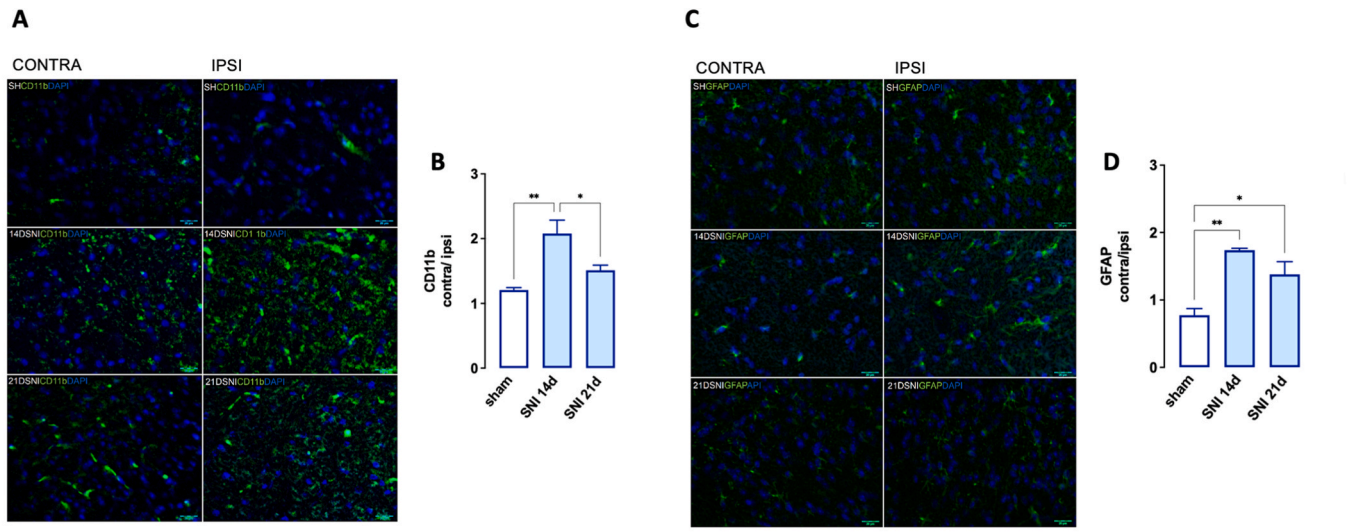

Fig. 6. Time-course of glial cell overexpression in the spinal cord of SNI mice. (A) Immunofluorescence micrographs showing the staining of microglia cells with the microglia marker CD11b in the contra and ipsilateral side of the spinal cord dorsal horn of SNI mice on day 14 and 21 post injury, Sham mice were used as control group. (B) Quantification analysis expressed as contra-ipsi ratio for CD11b immunostaining. (C) Immunofluorescence images for the staining of astroglial cells with the astrocyte marker GFAP in the contra and ipsilateral side of the spinal cord dorsal horn of SNI mice on day 14 and 21 post injury in comparison with sham mice. (B) Quantification analysis for GFAP immunostaining expressed as contra-ipsi ratio. Scale bar: 20 μm *p < 0.05 **p < 0.01 (one-way ANOVA).

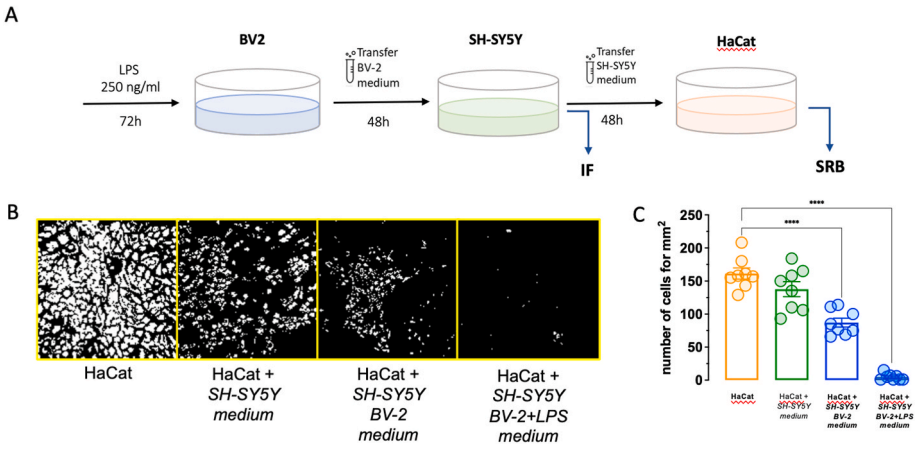

Fig. 7. Neuroinflammation-mediated toxicity on the epidermis in an in vitro model. (A) Schematic representation of the experimental protocol. (B) Representative images of HaCat exposed to SH-SH5Y medium obtained from unstimulated SH-SY5Y cells (SH-SY5Y medium), or cells exposed to unstimulated BV2-medium (BV2+SH-SH5Y) or exposed to LPS-simulated BV2 medium (LPS + BV2+SH-SH5Y), in comparison to unstimulated HaCat (CTRL) and (C) quantification of HaCat cell. Scale bar: 20 μm ***p < 0.001 ****p < 0.0001 (one-way ANOVA).

The number of HaCat exposed to the medium from unstimulated SH-SY5Y cells (SH-SY5Y *medium*), was unaltered. When keratinocytes were treated with the medium from BV-2 stimulated-SH-SY5Y (SH-SY5Y, BV2 *medium*) a significant decrease of viability was detected. The maximum toxicity in HaCat cells was observed after the stimulation with conditioned medium from SH-SY5Y, which were previously exposed to LPS-stimulated BV2 cell medium (SH-SY5Y, BV-2 +LPS *medium*) Fig. 7 B, C – No-cropped images are reported in Fig. 3 Supplementary).

4. Discussion

Neuropathic itch is an unpleasant sensation that affects a discrete amount of neuropathic pain suffering patients. This condition is often intractable and has a profound negative effect on patient's quality of life. Several experimental models have been proposed to study the pathophysiology of neuropathic itch (Brewer et al., 2008; Chen et al., 2022). Although they provided some important information, these models do not completely mimic molecular and cellular mechanisms of neuropathic itch. Indeed, they require the administration of pruritogen substances to induce a scratching behavior and do not fully recapitulate human disease conditions of spontaneous or mechanically evoked itch associated with neuropathic pain.

The present study aimed to characterize the itching phenotype of neuropathic mice through a time-course evaluation of spontaneous and mechanically evoked pruritus. We used the SNI model as peripheral neuropathies represent the most common etiology for neuropathic itch (Rosen et al., 2018). SNI male mice showed spontaneous scratching behavior. This itching phenotype appeared on day 7, peaked on day 14 and disappeared on day 21 post-injury. Interestingly, spontaneous itch was detectable in the morning but not in the evening. A plausible explanation for this circadian fluctuation of itch sensation may be related to the disruption by the neuropathy of physiological circadian patterns of some hormones or inflammatory mediators. Among others, a possible role for melatonin serum levels can be hypothesized. Melatonin

administration has been reported to reduce itch (Zhang et al., 2022) and SNI mice showed a reduced melatonin serum levels (Yang et al., 2018). Furthermore, changes in the circadian expression of melatonin receptors in the hypothalamus, with a drastic reduction in the morning and high levels in the evening, have been detected in mice after peripheral nerve injuries (Odo et al., 2014).

SNI mice showed hyperkinesis after application of a mechanical stimulus on the dorsal skin with a time-course overlapping that of spontaneous itch. Consistent with previous finding (Sanna et al., 2017), the same animals showed an intense and prolonged mechanical allodynia and thermal hyperalgesia that peaked on day 7 and remained unaltered up to 21 days after surgery. By comparing the itching and nociceptive behavior we observed that pain and itch overlapped in the early phases of the neuropathy, then itch attenuated while pain maintained a long-lasting pattern.

Several studies demonstrated a reduction in the quality of life in patients suffering from chronic itch, with the development of anxiety and depression, sensations which in turn lead to an exacerbation of the itch itself, creating a vicious circle (Sanders and Akiyama, 2018). During the evaluation of the itching profile, tests were carried out to verify the development of anxiety in mice. The results demonstrated a trend towards an increase in the anxiety-like behavior in SNI mice 14 days after the operation that further increased on day 21, as reported in previous studies (Borgonetti and Galeotti, 2023; Guida et al., 2020a). In addition to a correlation with pain hypersensitivity, present findings indicate a close relationship between itching and anxiety in this model of peripheral neuropathy.

Treatment with gabapentin and pregabalin, a first line treatment for neuropathic pain (Attal and Bouhassira, 2021) with some efficacy also in attenuating neuropathic itch (Auyeung et al., 2023), was able to reduce pain hypersensitivity as well as spontaneous and mechanically evoked itch, giving behavioral evidence of development of neuropathic itch in SNI mice. Both gabapentin and pregabalin showed a similar PK in male and female patients (Schmid et al., 2019). Notably, sex differences in chronic pain need to be further explored in depth for future therapeutical approach (Ahlström et al., 2021; Ann M Gregus et al., 2021). Several studies revealed that microglia are necessary for the development of neuropathic pain hypersensitivity in males but not in females (Brings and Zylka, 2015; Guida et al., 2020; Halievski et al., 2020; Sorge et al., 2015; Tansley et al., 2022). Therefore, we focused only on males, to correlate the development of neuropathic itch with microgliosis. However, the lack of data about female mice represents a limitation. Indeed, clinical data reported that women suffer more often from itch attacks, and they have more scratch lesions (Schmid et al., 2019) compared to men. Coherently, in an animal model of lymphoma female mice showed a higher number of scratching bouts compared to males (Chen et al., 2023). Therefore, the next step will be to better investigate the onset of neuropathy-associated pruritus in a model that is able to induce microgliosis and neuropathic pain symptoms in females and to promote the onset of pruritus.

We also provided further evidence to this hypothesis by histological analyses of the epidermis. IENFs are free nerve endings arising from Ad and/or C fibers from sensory neurons within the skin dermis and play a key role in the transmission of peripheral pain. A significant reduction in the IENFs density in the skin contributes to the neuropathic pain in humans (Mangus et al., 2020; Üçeyler et al., 2013) and IENFs analysis in skin biopsy samples represent a diagnostic tool for peripheral neuropathies in patients (Myers and Peltier, 2013). Several animal models of peripheral neuropathy are characterized by a loss of IENF density (Klazas et al., 2022; Ko et al., 2014; O'brien et al., 2014; Sanna et al., 2020), mimicking clinical states. A correlation between altered IENF density and chronic pruritus has also been postulated (Pereira et al., 2016). In conditions of inflammatory itch, the IENF is increased (Tominaga and Takamori, 2014; Xing et al., 2020) while in several models of neuropathic itch the IENF is decreased (Xu et al., 2023). This condition is also observed clinically in neuropathic itch suffering patients (Pereira et al., 2020), reflecting one pathogenic difference between inflammatory and neuropathic itch. Consistently, a reduction of the IENF density was detected on day 14, when the scratching behavior was fully established. Evidence indicates that release of proinflammatory molecules participates to neuropathic itch. After peripheral nerve injury, degenerating peripheral nerve fibers lead to release of inflammatory mediators and a significant inflammation develops along with appearance of sensory abnormalities (Davies et al., 2020). Itch neurons express a variety of receptors for inflammatory mediators (Chandran et al., 2016) and it is plausible that a component of neuropathic itch origins from the stimulation of the receptors of inflammatory molecules. SNI mice showed a proinflammatory response in the epidermis along with an increased epidermis thickness in coincidence with the scratching behavior, further indicating the presence of neuropathic itch.

Investigating into the signaling pathway involved in the itch processing, we highlighted a close connection between the skin and the central nervous system. In addition to peripheral skin sites, neuropathic itch involves other important peripheral and central neuronal sites such as DRG and spinal cord (Cevikbas and Lerner, 2020). Itch sensory neurons are cells that reside in the DRG and both innervate the skin and connect to the outer laminar layers of the spinal cord dorsal horn. These neurons synthesize and release itch neuropeptides, molecules that prominently contribute to the spinal processing of itch. SNI mice showed an increased protein expression of the itch neuropeptide BNP in spinal cord that temporally coincided with the scratching behavior, indicating a prominent role of this peptide in neuropathic itch processing. In the periphery, BNP expressing neurons are considered an itch-exclusive neuronal population. Injection of this peptide produces exclusive itch, and its ablation in mice produces specific itch deficits with intact pain (Mishra and Hoon, 2013). Furthermore, high BNP levels in the skin were described in inflammatory itch including atopic dermatitis (Meng et al., 2018), psoriasis suffering patients (Nattkemper et al., 2018) or animal models (Ewald et al., 2017; Liu et al., 2016). BNP released from sensory neurons has been reported to increase the release of IL-17 from keratinocytes (Meng et al., 2020). In various forms of chronic itching, such as atopic dermatitis and psoriasis, an increase in the expression of interleukins, especially IL-17, has been found at the skin level (Liu et al., 2020).

Further analysis on the role of BNP in neuropathic itch showed a spinal overexpression of this peptide that was observed in the dorsal horn, but not in the ventral horn, reflecting the anatomical location in lamina I of BNP-positive itch sensitive fibers (Mishra and Hoon, 2013). Indeed, it has been hypothesized that itch is transmitted through BNP-positive peripheral afferents contacting spinal dorsal horn neurons expressing BNP receptors. The BNP released from peripheral sensory neurons stimulates its receptors on gastrin releasing peptide (GRP)-positive second-order neurons to release GRP to stimulate third-order neurons expressing GRP receptors to transmit itch signal to the brain (Mishra and Hoon, 2013). An increased content of IL17 was detected in the spinal cord and DRG, along with an overexpression of pERK1/2, indicating a functional activation of the IL17-mediated pathway. These results provide some evidence for a BNP/IL17-mediated pathway for the transmission of pruritus at both peripheral and central level in SNI mice.

Alterations in microglia and astrocytes morphology and activity have been shown to play a role in neuropathic pain by promoting neuroinflammation. Growing evidence also indicates a role of glial cells in itch processing (Shiratori-Hayashi and Tsuda, 2021; Tsuda, 2018). Previous data highlighted the role of astrogliosis (Ji et al., 2019; Shiratori-Hayashi et al., 2021) and microgliosis (Sun et al., 2022; Yang et al., 2023) in the promotion of pain hypersensitivity in SNI mice. Present results showed an increased microglia and astrocyte activation in the spinal cord dorsal horns in the ipsilateral side of SNI mice in coincidence with the peak of scratching behavior, indicating a possible link between glial cell activation and sensory hypersensitivity. Results from in vitro

tests supported the hypothesis of a relationship among central and peripheral events through a BNP-mediated pathways. SH-SY5Y cells, exposed to the medium from LPS-stimulated BV2 cells, showed an increase in the BNP expression. Stimulation of HaCat cells with the SH-SY5Y medium dramatically reduced HaCat cell viability. Conversely, exposure of HaCat to unstimulated SH-SY5Y medium did not produce any effect, hypothesizing that neuropathic itch may depend on glia-mediated neuroinflammation mechanism at the spinal cord level, that then affects neurons activity and consequently skin epidermis events.

5. Conclusions

In conclusion, present study showed the development of spontaneous neuropathic itch in SNI mice. Through a behavioral, histological, and biological characterization of the SNI-associated scratching phenotype, we hypothesized an initiation of the itch sensation by the release of BNP in the spinal cord because of the injury-induced neuroinflammation. The definition of the time-course of spontaneous and mechanically evoked scratching behavior and of associated molecular events provided by the present study might represent a starting point for testing new therapeutic intervention for neuropathic itch using on SNI.

CRediT authorship contribution statement

Vittoria Borgonetti: Methodology, Investigation, Formal analysis, Data curation. **Martina Morozzi:** Investigation, Formal analysis. **Nicoletta Galeotti:** Writing – original draft, Supervision, Project administration, Data curation, Conceptualization.

Declaration of competing interest

The authors have no conflicts of interest to declare.

Data availability

Data will be made available on request.

Acknowledgments

Supported by grants from the University of Florence.

Appendix A. Supplementary data

Supplementary data to this article can be found online at https://doi.org/10.1016/j.neuropharm.2024.110120.

References

Ahlström, F.H.G., Mätlik, & K., Viisanen, H., Blomqvist, K.J., Liu, X., Lilius, T.O., Sidorova, Y., Kalso, E.A., Rauhala, P.V., 2021. Spared nerve injury causes sexually dimorphic mechanical allodynia and differential gene expression in spinal cords and dorsal root ganglia in rats. Molecular Neuropbiology 58, 5396–5419. https://doi.org/10.1007/s12035-021-02447-1/Published.

Andersen, H.H., Akiyama, T., Nattkemper, L.A., Van Laarhoven, A., Elberling, J., Yosipovitch, G., Arendt-Nielsen, L., 2018. Alloknesis and hyperknesis-mechanisms, assessment methodology, and clinical implications of itch sensitization. Pain 159, 1185–1197. https://doi.org/10.1097/J.PAIN.0000000000001220.

Attal, N., Bouhassira, D., 2021. Advances in the treatment of neuropathic pain. Curr. Opin. Neurol. 34, 631–637. https://doi.org/10.1097/WCO.0000000000000980.

Auyeung, K.L., Jenkins, B.A., Kim, B.S., 2023. Clinical management of neuropathic itch. JAMA Dermatol 159. https://doi.org/10.1001/JAMADERMATOL.2023.3384.

Basbaum, A.I., Bautista, D.M., Scherrer, G., Julius, D., 2009. Cellular and molecular mechanisms of pain. Cell 139, 267–284. https://doi.org/10.1016/j.cell.2009.09.028.

Borgonetti, V., Galeotti, N., 2023. Microglia senescence is related to neuropathic pain-associated comorbidities in the spared nerve injury model. Pain 164, 1106–1117. https://doi.org/10.1097/J.PAIN.0000000000002807.

Borgonetti, V., Galeotti, N., 2021. Intranasal delivery of an antisense oligonucleotide to the RNA-binding protein HuR relieves nerve injury-induced neuropathic pain. Pain 162, 1500–1510. https://doi.org/10.1097/j.pain.0000000000002154.

Brewer, K.L., Lee, J.W., Downs, H., Oaklander, A.L., Yezierski, R.P., 2008. Dermatomal scratching after intramedullary quisqualate injection: correlation with cutaneous denervation. J. Pain 9, 999–1005. https://doi.org/10.1016/J.JPAIN.2008.05.010.

Brings, V.E., Zylka, M.J., 2015. Sex, drugs and pain control. Nat. Neurosci. https://doi.org/10.1038/nn.4057.

Bushnell, M.C., Ceko, M., Low, L.A., 2013. Cognitive and emotional control of pain and its disruption in chronic pain. Nat. Rev. Neurosci. 14, 502–511. https://doi.org/10.1038/NRN3516.

Cevikbas, F., Lerner, E.A., 2020. Physiology and pathophysiology of itch. Physiol. Rev. 100, 945–982. https://doi.org/10.1152/PHYSREV.00017.2019.

Chandran, V., Coppola, G., Nawabi, H., Omura, T., Versano, R., Huebner, E.A., Zhang, A., Costigan, M., Yekkirala, A., Barrett, L., Blesch, A., Michaelevski, I., Davis-Turak, J., Gao, F., Langfelder, P., Horvath, S., He, Z., Benowitz, L., Fainzilber, M., Tuszynski, M., Woolf, C.J., Geschwind, D.H., 2016. A systems-level analysis of the peripheral nerve intrinsic axonal growth program. Neuron 89, 956–970. https://doi.org/10.1016/J.NEURON.2016.01.034.

Charan, J., Kantharia, N., 2013. How to calculate sample size in animal studies? J. Pharmacol. Pharmacother. 4, 303–306. https://doi.org/10.4103/0976-500X.119726.

Chen, O., He, Q., Han, Q., Furutani, K., Gu, Y., Olexa, M., Ji, R.R., 2023. Mechanisms and treatments of neuropathic itch in a mouse model of lymphoma. J. Clin. Invest. 133 https://doi.org/10.1172/JCI160807.

Chen, Y., Song, Y., Wang, H., Zhang, Y., Hu, X., Wang, K., Lu, Y., Zhang, Z., Li, S., Li, A., Bao, L., Xu, F., Li, C., Zhang, X., 2022. Distinct neural networks derived from galanin-containing nociceptors and neurotensin-expressing pruriceptors. Proc. Natl. Acad. Sci. U. S. A. 119 https://doi.org/10.1073/PNAS.2118501119.

Davies, A.J., Rinaldi, S., Costigan, M., Oh, S.B., 2020. Cytotoxic immunity in peripheral nerve injury and pain. Front. Neurosci. 14 https://doi.org/10.3389/FNINS.2020.00142.

Decosterd, I., Woolf, C.J., 2000. Spared nerve injury: an animal model of persistent peripheral neuropathic pain. Pain 87.

Dick, B.D., Rashiq, S., 2007. Disruption of attention and working memory traces in individuals with chronic pain. Anesth. Analg. 104, 1223–1229. https://doi.org/10.1213/01.ANE.0000263280.49786.F5.

Ewald, D.A., Noda, S., Oliva, M., Litman, T., Nakajima, S., Li, X., Xu, H., Workman, C.T., Scheipers, P., Svitacheva, N., Labuda, T., Krueger, J.G., Suárez-Fariñas, M., Kabashima, K., Guttman-Yassky, E., 2017. Major differences between human atopic dermatitis and murine models, as determined by using global transcriptomic profiling. J. Allergy Clin. Immunol. 139, 562–571. https://doi.org/10.1016/J.JACI.2016.08.029.

Finnerup, N.B., Kuner, R., Jensen, T.S., 2021. Neuropathic pain: from mechanisms to treatment. Physiol. Rev. 101, 259–301. https://doi.org/10.1152/physrev.00045.2019.

Galeotti, N., Ghelardini, C., Zoppi, M., Del Bene, E., Raimondi, L., Beneforti, E., Bartolini, A., 2001. Hypofunctionality of Gi proteins as aetiopathogenic mechanism for migraine and cluster headache. Cephalalgia 21, 38–45. https://doi.org/10.1046/j.1468-2982.2001.00142.x.

Gregus, Ann M., Levine, I.S., Eddinger, K.A., Yaksh, T.L., Buczynski, M.W., 2021. Sex differences in neuroimmune and glial mechanisms of pain. Pain. https://doi.org/10.1097/j.pain.0000000000002215.

Guida, F., De Gregorio, D., Palazzo, E., Ricciardi, F., Boccella, S., Belardo, C., Iannotta, M., Infantino, R., Formato, F., Marabese, I., Luongo, L., de Novellis, V., Maione, S., 2020. Behavioral, biochemical and electrophysiological changes in spared nerve injury model of neuropathic pain. Int. J. Mol. Sci. 21 https://doi.org/10.3390/IJMS21093396.

Hachisuka, J., Chiang, M.C., Ross, S.E., 2018. Itch and neuropathic itch. Pain. https://doi.org/10.1097/j.pain.0000000000001141.

Halievski, K., Ghazisaeidi, S., Salter, M.W., 2020. Sex-dependent mechanisms of chronic pain: a focus on microglia and p2x4r. J. Pharmacol. Exp. Therapeut. https://doi.org/10.1124/JPET.120.265017.

Ikoma, A., Steinhoff, M., Ständer, S., Yosipovitch, G., Schmelz, M., 2006. The neurobiology of itch. Nat. Rev. Neurosci. 7, 535–547. https://doi.org/10.1038/nrn1950.

Ji, R.R., Donnelly, C.R., Nedergaard, M., 2019. Astrocytes in chronic pain and itch. Nat. Rev. Neurosci. https://doi.org/10.1038/s41583-019-0218-1.

Klazas, M., Naamneh, M.S., Zheng, W., Lazarovici, P., 2022. Gabapentin increases intraepidermal and peptidergic nerve fibers density and alleviates allodynia and thermal hyperalgesia in a mouse model of acute taxol-induced peripheral neuropathy. Biomedicines 10. https://doi.org/10.3390/BIOMEDICINES10123190.

Ko, M.H., Hu, M.E., Hsieh, Y.L., Lan, C.T., Tseng, T.J., 2014. Peptidergic intraepidermal nerve fibers in the skin contribute to the neuropathic pain in paclitaxel-induced peripheral neuropathy. Neuropeptides 48, 109–117. https://doi.org/10.1016/J.NPEP.2014.02.001.

Liu, B., Tai, Y., Achanta, S., Kaelberer, M.M., Caceres, A.I., Shao, X., Fang, J., Jordt, S.E., 2016. IL-33/ST2 signaling excites sensory neurons and mediates itch response in a mouse model of poison ivy contact allergy. Proc. Natl. Acad. Sci. U. S. A. 113, E7572–E7579. https://doi.org/10.1073/PNAS.1606608113.

Liu, T., Ji, R.R., 2013. New insights into the mechanisms of itch: are pain and itch controlled by distinct mechanisms? Pflügers Archiv 465, 1671–1685. https://doi.org/10.1007/S00424-013-1284-2.

Liu, T., Li, S., Ying, S., Tang, S., Ding, Y., Li, Y., Qiao, J., Fang, H., 2020. The IL-23/IL-17 pathway in inflammatory skin diseases: from bench to bedside. Front. Immunol. 11 https://doi.org/10.3389/FIMMU.2020.594735.

Ma, Q., 2022. A functional subdivision within the somatosensory system and its implications for pain research. Neuron 110, 749–769. https://doi.org/10.1016/J.NEURON.2021.12.015.

Mangus, L.M., Rao, D.B., Ebenezer, G.J., 2020. Intraepidermal nerve fiber analysis in human patients and animal models of peripheral neuropathy: a comparative review. Toxicol. Pathol. 48, 59–70. https://doi.org/10.1177/0192623319855969.
Matsuda, K.M., Sharma, D., Schonfeld, A.R., Kwatra, S.G., 2016. Gabapentin and pregabalin for the treatment of chronic pruritus. J. Am. Acad. Dermatol. 75, 619–625.e6. https://doi.org/10.1016/J.JAAD.2016.02.1237.
Meng, J., Chen, W., Wang, J., 2020. Interventions in the B-type natriuretic peptide signalling pathway as a means of controlling chronic itch. Br. J. Pharmacol. 177, 1025–1040. https://doi.org/10.1111/BPH.14952.
Meng, J., Moriyama, M., Feld, M., Buddenkotte, J., Buhl, T., Szöllösi, A., Zhang, J., Miller, P., Ghetti, A., Fischer, M., Reeh, P.W., Shan, C., Wang, J., Steinhoff, M., 2018. New mechanism underlying IL-31-induced atopic dermatitis. J. Allergy Clin. Immunol. 141, 1677–1689.e8. https://doi.org/10.1016/J.JACI.2017.12.1002.
Mishra, S.K., Hoon, M.A., 2013. The cells and circuitry for itch responses in mice. Science 340, 968–971. https://doi.org/10.1126/SCIENCE.1233765.
Myers, M.I., Peltier, A.C., 2013. Uses of skin biopsy for sensory and autonomic nerve assessment. Curr. Neurol. Neurosci. Rep. 13 https://doi.org/10.1007/S11910-012-0323-2.
Nattkemper, L.A., Tey, H.L., Valdes-Rodriguez, R., Lee, H., Mollanazar, N.K., Albornoz, C., Sanders, K.M., Yosipovitch, G., 2018. The genetics of chronic itch: gene expression in the skin of patients with atopic dermatitis and psoriasis with severe itch. J. Invest. Dermatol. 138, 1311–1317. https://doi.org/10.1016/J.JID.2017.12.029.
Oaklander, A.L., Bowsher, D., Galer, B., Haanpää, M., Jensen, M.P., 2003. Herpes zoster itch: preliminary epidemiologic data. J. Pain 4, 338–343. https://doi.org/10.1016/S1526-5900(03)00637-0.
O'brien, P.D., Sakowski, S.A., Feldman, E.L., 2014. Mouse models of diabetic neuropathy. ILAR J. 54, 259–272. https://doi.org/10.1093/ILAR/ILT052.
Odo, M., Koh, K., Takada, T., Yamashita, A., Narita, Michiko, Kuzumaki, N., Ikegami, D., Sakai, H., Iseki, M., Inada, E., Narita, Minoru, 2014. Changes in circadian rhythm for mRNA expression of melatonin 1A and 1B receptors in the hypothalamus under a neuropathic pain-like state. Synapse 68, 153–158. https://doi.org/10.1002/SYN.21728.
Pereira, M.P., Derichs, L., Meyer Zu Hörste, G., Agelopoulos, K., Ständer, S., 2020. Generalized chronic itch induced by small-fibre neuropathy: clinical profile and proposed diagnostic criteria. J. Eur. Acad. Dermatol. Venereol. 34, 1795–1802. https://doi.org/10.1111/JDV.16151.
Pereira, M.P., Mühl, S., Pogatzki-Zahn, E.M., Agelopoulos, K., Ständer, S., 2016. Intraepidermal nerve fiber density: diagnostic and therapeutic relevance in the management of chronic pruritus: a review. Dermatol. Ther. 6, 509–517. https://doi.org/10.1007/S13555-016-0146-1.
Poddar, S., Mondal, H., Podder, I., 2023. Aetiology, pathogenesis and management of neuropathic itch: a narrative review with recent updates. Indian J. Dermatol. Venereol. Leprol. 1–14. https://doi.org/10.25259/IJDVL_846_2022.
Rayner, L., Hotopf, M., Petkova, H., Matcham, F., Simpson, A., Mccracken, L.M., 2016. Depression in patients with chronic pain attending a specialised pain treatment centre: prevalence and impact on health care costs. Pain 157, 1472–1479. https://doi.org/10.1097/J.PAIN.0000000000000542.
Rosen, J.D., Fostini, A.C., Yosipovitch, G., 2018. Diagnosis and management of neuropathic itch. Dermatol. Clin. 36, 213–224. https://doi.org/10.1016/J.DET.2018.02.005.
Sanders, K.M., Akiyama, T., 2018. The vicious cycle of itch and anxiety. Neurosci. Biobehav. Rev. 87, 17–26. https://doi.org/10.1016/J.NEUBIOREV.2018.01.009.
Sanna, M.D., Lucarini, L., Durante, M., Ghelardini, C., Masini, E., Galeotti, N., 2017. Histamine H4 receptor agonist-induced relief from painful peripheral neuropathy is mediated by inhibition of spinal neuroinflammation and oxidative stress. Br. J. Pharmacol. 174, 28–40. https://doi.org/10.1111/bph.13644.
Sanna, M.D., Manassero, G., Vercelli, A., Herdegen, T., Galeotti, N., 2020. The isoform-specific functions of the c-Jun N-terminal kinase (JNK) in a mouse model of antiretroviral-induced painful peripheral neuropathy. Eur. J. Pharmacol. 880 https://doi.org/10.1016/J.EJPHAR.2020.173161.
Sanna, M.D., Mello, T., Masini, E., Galeotti, N., 2018. Activation of ERK/CREB pathway in noradrenergic neurons contributes to hypernociceptive phenotype in H4 receptor knockout mice after nerve injury. Neuropharmacology 128, 340–350. https://doi.org/10.1016/j.neuropharm.2017.10.025.
Schmid, Y., Navarini, A., Thomas, Z.R.M., Pfleiderer, B., Krähenbühl, S., Mueller, S.M., 2019. Sex differences in the pharmacology of itch therapies—a narrative review. Curr. Opin. Pharmacol. https://doi.org/10.1016/j.coph.2019.05.008.
Shiratori-Hayashi, M., Tsuda, M., 2021. Spinal glial cells in itch modulation. Pharmacol Res Perspect 9. https://doi.org/10.1002/PRP2.754.
Shiratori-Hayashi, M., Yamaguchi, C., Eguchi, K., Shiraishi, Y., Kohno, K., Mikoshiba, K., Inoue, K., Nishida, M., Tsuda, M., 2021. Astrocytic STAT3 activation and chronic itch require IP3R1/TRPC-dependent Ca2+ signals in mice. J. Allergy Clin. Immunol. 147, 1341–1353. https://doi.org/10.1016/j.jaci.2020.06.039.
Sorge, R.E., Mapplebeck, J.C.S., Rosen, S., Beggs, S., Taves, S., Alexander, J.K., Martin, L. J., Austin, J.S., Sotocinal, S.G., Chen, D., Yang, M., Shi, X.Q., Huang, H., Pillon, N.J., Bilan, P.J., Tu, Y., Klip, A., Ji, R.R., Zhang, J., Salter, M.W., Mogil, J.S., 2015. Different immune cells mediate mechanical pain hypersensitivity in male and female mice. Nat. Neurosci. 18, 1081–1083. https://doi.org/10.1038/nn.4053.
Ständer, S., Grundmann, S.A., 2013. Clinical practice. Chronic pruritus. N. Engl. J. Med. 368, 161–169. https://doi.org/10.1056/NEJMCP1208814.
Steinhoff, M., Bienenstock, J., Schmelz, M., Maurer, M., Wei, E., Bíró, T., 2006. Neurophysiological, neuroimmunological, and neuroendocrine basis of pruritus. J. Invest. Dermatol. 126, 1705–1718. https://doi.org/10.1038/SJ.JID.5700231.
Steinhoff, M., Schmelz, M., Szabó, I.L., Oaklander, A.L., 2018. Clinical presentation, management, and pathophysiology of neuropathic itch. Lancet Neurol. 17, 709–720. https://doi.org/10.1016/S1474-4422(18)30217-5.
Stumpf, A., Ständer, S., 2013. Neuropathic itch: diagnosis and management. Dermatol. Ther. 26, 104–109. https://doi.org/10.1111/DTH.12028.
Sun, J., Zhou, Y. qun, Xu, B. yang, Li, J. yan, Zhang, L. qing, Li, D. yang, Zhang, S., Wu, J. yi, Gao, S. jie, Ye, D. wei, Mei, W., 2022. STING/NF-κB/IL-6-Mediated inflammation in microglia contributes to spared nerve injury (SNI)-Induced pain initiation. J. Neuroimmune Pharmacol. 17, 453–469. https://doi.org/10.1007/S11481-021-10031-6.
Tansley, S., Uttam, S., Ureña Guzmán, A., Yaqubi, M., Pacis, A., Parisien, M., Deamond, H., Wong, C., Rabau, O., Brown, N., Haglund, L., Ouellet, J., Santaguida, C., Ribeiro-da-Silva, A., Tahmasebi, S., Prager-Khoutorsky, M., Ragoussis, J., Zhang, J., Salter, M.W., Diatchenko, L., Healy, L.M., Mogil, J.S., Khoutorsky, A., 2022. Single-cell RNA sequencing reveals time- and sex-specific responses of mouse spinal cord microglia to peripheral nerve injury and links ApoE to chronic pain. Nat. Commun. 13 https://doi.org/10.1038/s41467-022-28473-8.
Tominaga, M., Takamori, K., 2014. Itch and nerve fibers with special reference to atopic dermatitis: therapeutic implications. J. Dermatol. 41, 205–212. https://doi.org/10.1111/1346-8138.12317.
Tsuda, M., 2018. Modulation of pain and itch by spinal glia. Neurosci. Bull. 34, 178–185. https://doi.org/10.1007/S12264-017-0129-Y.
Üçeyler, N., Zeller, D., Kahn, A.K., Kewenig, S., Kittel-Schneider, S., Schmid, A., Casanova-Molla, J., Reiners, K., Sommer, C., 2013. Small fibre pathology in patients with fibromyalgia syndrome. Brain 136, 1857–1867. https://doi.org/10.1093/BRAIN/AWT053.
Wimalasena, N.K., Milner, G., Silva, R., Vuong, C., Zhang, Z., Bautista, D.M., Woolf, C.J., 2021. Dissecting the precise nature of itch-evoked scratching. Neuron 109, 3075–3087.e2. https://doi.org/10.1016/J.NEURON.2021.07.020.
Woo, A.K., 2010. Depression and anxiety in pain. Rev Pain 4, 8–12. https://doi.org/10.1177/204946371000400103.
Xing, Y., Chen, J., Hilley, H., Steele, H., Yang, J., Han, L., 2020. Molecular signature of pruriceptive MrgprA3+ neurons. J. Invest. Dermatol. 140, 2041–2050. https://doi.org/10.1016/J.JID.2020.03.935.
Xu, J. wen, Xu, X., Ling, Y., Wang, Y. chun, Huang, Y. jie, Yang, J. zhen, Wang, J. ying, Shen, X., 2023. Vincamine as an agonist of G-protein-coupled receptor 40 effectively ameliorates diabetic peripheral neuropathy in mice. Acta Pharmacol. Sin. 44 https://doi.org/10.1038/S41401-023-01135-1.
Yang, Y., Mou, B., Zhang, Q.R., Zhao, H.X., Zhang, J.Y., Yun, X., Xiong, M.T., Liu, Y., Liu, Y.U., Pan, H., Ma, C.L., Li, B.M., Peng, J., 2023. Microglia are involved in regulating histamine-dependent and non-dependent itch transmissions with distinguished signal pathways. Glia 71, 2541–2558. https://doi.org/10.1002/glia.24438.
Yang, Z., Li, C., Wang, Y., Yang, J., Yin, Y., Liu, M., Shi, Z., Mu, N., Yu, L., Ma, H., 2018. Melatonin attenuates chronic pain related myocardial ischemic susceptibility through inhibiting RIP3-MLKL/CaMKII dependent necroptosis. J. Mol. Cell. Cardiol. 125, 185–194. https://doi.org/10.1016/J.YJMCC.2018.10.018.
Zhang, L., Zhang, J.-T., Huang, Y., Zhou, G.-K., Zhou, Y., Yang, J.-P., Liu, T., 2022. Melatonin attenuates acute and chronic itch in mice: the antioxidant and anti-inflammatory effects of melatonin receptors. Ann. Transl. Med. 10, 972. https://doi.org/10.21037/ATM-22-3804, 972.